Electrically evoked otoacoustic emissions from the apical turns of the gerbil cochlea

Hideko H. Nakajima and Elizabeth S. Olson
Department of Biomedical Engineering, Boston University, Boston, Massachusetts 02215

David C. Mountain
Departments of Biomedical Engineering and Otolaryngology, Boston University, Boston, Massachusetts 02215

Allyn E. Hubbard
Departments of Biomedical Engineering, Electrical, Computer, and Systems Engineering, and Otolaryngology, Boston University, Boston, Massachusetts 02215

Electrically evoked otoacoustic emissions were measured with current delivered to the second and third turns of the gerbil cochlea. The emission magnitude and phase are dependent on the characteristic frequency (CF) of the stimulating microelectrode location. The death of the animal resulted in an initial increase in emission below the CF of the electrode location and a decrease in emission near the CF of the electrode location. The group delay of the electrically evoked emission phase data is twice as large as the acoustically evoked cochlear microphonic (CM) data obtained by Schmiedt and Zwislocki [J. Acoust. Soc. Am. **61**, 133–149 (1977)]. This suggests the possibility of two separate propagation modes for the forward and reverse traveling waves.

INTRODUCTION

The frequency selectivity of the basilar membrane (indicated by the shape of the tuning curve measured at fixed positions) for low-level sound stimuli is extremely high, but rapidly declines with the death of an animal (Rhode, 1971, 1973, 1978; Sellick *et al.*, 1982). It is likely in live animals that such selectivity is produced by an active process requiring energy (see Davis, 1983). The active process is hypothesized to modify or amplify the local mechanical response of the cochlea. Isolated cochlear outer hair cells (OHC) from the mammalian cochlea have been shown to exhibit voltage-dependent length changes (Brownell *et al.*, 1985; Ashmore, 1987). Because of this ability, OHCs are thought to be part of the active process.

Hubbard and Mountain (1983) and Mountain *et al.* (1983) have shown that intracochlear electrical stimulation produces pressure, measurable at the eardrum. This pressure, termed the electrically evoked otoacoustic emission, may be generated by the motion of the OHCs, thus reflecting the active process. Recently Xue *et al.* (1993b) measured basilar membrane motion, also evoked by sinusoidal current injected into the scala media. He compared and showed similarities between the electrically evoked emission and the electrically evoked basilar membrane motion measurements for various frequencies in the same cochlea. Measurements of the electrically evoked emission and the electrically evoked basilar membrane motion were consistent with the hypothesis that OHC voltage-dependent length changes are responsible for basilar membrane motion. By studying the cochlea's ability to produce acoustic responses to electrical current stimuli, we can explore the electromotility present in the intact cochlea.

Mountain and Hubbard (1989) reported that the frequency response of the electrically evoked emissions depended on the location of the stimulating electrode. They showed that for current injected into the first and second turns of the gerbil, the cutoff frequency for the emission was approximately two octaves below the estimated CF. More recently, Murata *et al.* (1991) reported similar electrically evoked emission-magnitude frequency responses with low-pass characteristics. They found that cutoff frequencies in the second and third turns of the guinea pig were close to the estimated CF of the electrode location.

The difference in cutoff frequency may be attributable, all or in part, to species differences, cochlear condition, acoustic load, or stimulation technique. To extend our knowledge of electrically evoked emissions in the gerbil as well as addressing the source of the differences in these two reports, we have measured the emission magnitude and phase produced by the current delivered to the second and third turns of the gerbil under varying circumstances. Measurements were made with differing acoustic loads, as well as before and immediately after the death of the animal. We carefully monitored cochlear condition and minimized potential artifacts.

Analysis of the phase data uncovered an unexpected result. We find that, for frequencies below the CF of the electrode location, the group delays measured for the electrically evoked emissions are significantly greater than the corresponding group delays reported for the CM (Schmiedt and Zwislocki, 1977). The difference in group delays suggest that electrical and acoustic stimulation may stimulate different traveling-wave propagation modes.

I. METHODS

The experiments were performed on young adult Mongolian gerbils, *Meriones unguiculatus*, ranging in weight from 38–59 g. Each animal was initially given a preanesthetic, acepromazine (1 mg/kg), delivered intramuscularly, followed with sodium pentobarbital (Nembutal, 60 mg/kg), intraperitoneally. Supplemental sodium pentobarbital (12 mg/kg) was administered approximately every 20 to 30 min. The temperature of the gerbil was maintained at 38 °C. The pinnae were removed and a tracheotomy was performed. The gerbil's head was firmly secured with cyanoacrylate glue to a stereotaxic head holder. The ventro-lateral aspect of the left bulla was exposed and then opened to allow access to the round window and the second or third turn of the cochlea.

After the area surrounding the bony ear-canal opening was cleared and dried, the ear bar was glued to the ear-canal opening. Attached to the side of the ear bar was a 2-mm probe tube connected to a $\frac{1}{2}$-in. Brüel & Kjær microphone (type 4166). The distal end of the ear bar was connected through a tube approximately 7 cm long to a Beyer DT-48 earphone. The microphone and earphone were electrically isolated from each other and from the ear bar. Moisture was minimized around the bony ear-canal opening to ensure electrical isolation between the animal and the microphone.

Recordings of the eighth-nerve compound action potentials (N_1) were made with an insulated silver wire electrode with the exposed tip touching the bony surface of the cochlea near the round window. A subcutaneous Ag/AgCl reference electrode was placed anteriorly to the opened bulla. To minimize CM contamination, the stimulus tone bursts (6.4 ms with 1-ms rise times) were randomized in phase. Threshold rejection was applied to prevent the inclusion of large electrocardiographic signals in the recordings. The averaged compound action potential waveform was stored and the amplitude of the N_1 waveform was calculated. After obtaining the magnitudes for N_1 for a range of intensities and frequencies of stimuli (10 to 80 dB, 400 Hz to 20 kHz), the data was simplified by calculating the N_1 threshold at each frequency. The N_1 threshold was the intensity of sound required to produce an N_1 magnitude of a specified value within the range of 5 to 15 μV. The threshold was calculated by interpolating between the sound pressure levels used. The emission data presented here are from healthy cochleas exhibiting less than 7 dB of N_1-threshold shift after microelectrode insertion.

A small hole on the lateral wall of the cochlea was made gently by hand with a needle having a sharp point. A glass microelectrode inserted through the stria vascularis and into the scala media of either turn 3 or turn 2 was used both to record the electrical activity of the cochlea and to stimulate the cochlea with electrical current. To make a microelectrode, a glass capillary was pulled and the tip was fractured to a 2- to 4-μm diameter. The microelectrode was then filled with 1.5-M KCl solution resulting in an electrode impedance between 1 and 2 MΩ. An insulated silver wire, with a 3-mm silver-chlorided tip, was inserted into the KCl solution at the upper shank of the glass microelectrode. The entire microelectrode surface was electrically shielded with silver paint except for a 4-mm section exposed at the tip. A computer-controlled switch changed the microelectrode from the
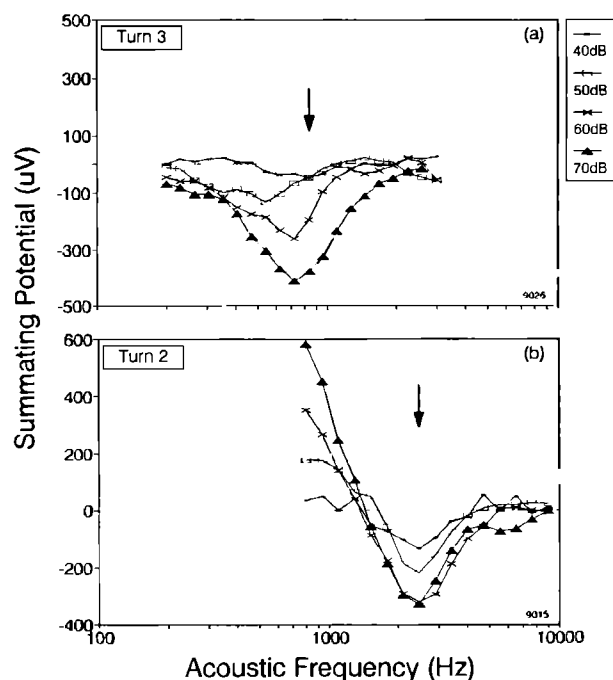
FIG. 1. Summating potential responses as a function of acoustic frequency and sound-pressure level for turn-2 and turn-3 experiments. The arrows indicate the estimates of the characteristic frequencies of the microelectrode locations based on the presented data.

current-stimulation mode to the voltage-recording mode.

In the voltage-recording mode, the microelectrode was used to measure the scala-media CM, the endocochlear potential (EP) and the summating potential (SP). A Ag/AgCl electrode, placed subcutaneously on the contralateral side near the trachea, was used as a reference for the voltage recordings. The steady-state response of the CM was averaged and stored. The EP was recorded as the dc potential in the scala media relative to the potential on the outer surface of the stria vascularis. The EP was measured when the microelectrode was first inserted into the scala media and again at the end of the experiment, when the microelectrode was withdrawn from the scala media. The presented data are from animals with high EP (64 to 98 mV), with the exception of the death study.

To determine the CF at the electrode location, the frequency response of the SP was measured. Acoustic stimulation near the CF results in a depolarization of the basal inner hair cells (Russell and Sellick, 1978; Cody and Russell, 1987; Kössl and Russell, 1992), and of the apical inner and outer hair cells (Dallos *et al.*, 1982; Dallos, 1985, 1986). Depolarization of these hair cells produces a local extracellular negative dc potential in the scala media, the negative SP. Therefore, the stimulus frequency that evoked the most negative SP was considered the CF of the hair cells near the electrode location. The CF of the electrode location was estimated by choosing the frequency of the peak negative SP response at relatively low-sound-pressure levels (40 to 60 dB SPL). When the electrode was located in the third turn of the cochlea, the CF was approximately 800 Hz [Fig. 1(a)]. The second turn region (basal to turn 3) had CFs between 2 and 3 kHz [Fig. 1(b)].

The microelectrode used to measure the electrical potential in the scala media was also used to stimulate the cochlea with ac current. An optically isolated, battery-operated stimulator was used to stimulate the scala media with alternating current ranging from 10 to 15 μA_{p-p}. The stimulator was driven by a programmable frequency synthesizer. For the return path of the current, a Ag/AgCl electrode was inserted under the skin between the neck and the contralateral ear. The current was monitored by measuring the voltage across a 100-Ω resistor in series with the return electrode. A constant current level was established for each experiment and verified by oscilloscope readings during the experiment. The microelectrode shield was connected to the return terminal of the current stimulator to prevent capacitive current from contaminating the current measurements.

Electrically evoked otoacoustic emissions at the stimulus current frequency were measured with the microphone. Stimulus frequencies for all steady-state recordings were set as close as possible to the desired frequencies while allowing integer numbers of cycles in a sampling window. The sample window was 17.0 ms for the emission measurements and 20.5 ms for the CM measurements. The steady-state portion of the emission and CM responses were processed using fast Fourier transform. Because the microphone response measurements contained low-frequency noise (not attenuated by the sound chamber or the high-pass filters), a Hanning window was applied to the data before performing a fast Fourier transform. The Hanning window was used to reduce spectral splatter from the low-frequency noise. Emission recordings were corrected for the probe-tube frequency response. The magnitude and phase of the component at the frequency of the stimulus current were then extracted. The phase of the emission (re: condensation) was calculated with respect to the injected current phase (re: positive current in the scala media).

Several steps were taken to ensure that the measurements of the electrically evoked emissions were free of artifacts. Electrical isolation had to be achieved at all locations between the stimulus signal and the equipment used to measure the emission. A check for electrical isolation between the probe tube and the ear bar was made approximately every hour during an experiment using an ohmmeter. To check for capacitive coupling between the stimulus system and the probe-tube microphone, we made a "surface" recording which measured the acoustic response to current stimulation with the microelectrode tip positioned on the surface of the bulla. In this case the current passed through the animal, but not the sensory hair cells within the cochlea. In addition, a "noise" recording was made by obtaining a frequency response without electrical stimulus signals. For the data reported here, the surface recordings were at the noise level.

For some electrically evoked emission measurements, we used a "blocked" ear-bar configuration: the earphone with its tubing was removed from the ear bar and the opening at the ear bar was blocked with a tight-fitting plastic-coated metal plug. After the earphone and tubing were removed and the ear bar blocked, the volume of the acoustic system was reduced from a volume of 0.75 to 0.03 cm^3.

Previous studies have noted effects of the acoustic load on the acoustically evoked distortion product emissions in the cat (Matthews, 1983; Fahey and Allen, 1985) and human (Zwicker, 1990). Reducing the volume of the acoustic load from the connected-earphone (unblocked) to the blocked ear bar affected the electrically evoked emission frequency response significantly (Fig. 2). Notches in the magnitude response occurred at approximately the same frequencies in the unblocked and blocked situations. However, the depth of most notches in the magnitude response was reduced in the blocked case. The difference between the two acoustic configurations was similar for turn-3 and turn-2 experiments. The change in emission measurements between the two configurations (the blocked relative to the unblocked) is plotted for turn 3 and turn 2 in Fig. 3. The observed increase in magnitude at low frequencies (below 250 Hz) for the blocked configuration is expected because of the decrease in compliance produced by the smaller volume. For the midfrequency region (300 to 500 Hz), both the turn-3 and turn-2 data showed that blocking the ear bar actually reduced the magnitude. Thus the positive hump in the magnitude frequency response at this frequency region for the unblocked configuration was reduced by blocking the ear bar. At higher frequencies (above 600 Hz), blocking the ear bar reduced the large notches in the magnitude response, resulting in increased emission magnitudes at the frequency of the notches. The phase responses of the unblocked and blocked situations were quite similar, except at frequencies below 500 Hz, where the blocked case resulted in phase that lagged more than the unblocked phase.

The origin of the local maximum of the magnitude frequency response at midfrequencies and the large notches at high frequencies, with the earphone attached, is unclear. If the notches were due to resonances in the acoustic system with the earphone and the tube attached, then the notches would be expected at frequencies where multiples of half-wavelengths occur in the tube. The length of the earphone tubing plus ear bar from earphone to ear canal was approximately 11 cm. The resonant frequency would then be expected to occur at $\lambda/2 \approx 1.6$ kHz, $\lambda \approx 3.1$ kHz, and $(3^*\lambda)/2 \approx 4.7$ kHz. These frequencies are similar, but not identical to the frequencies where the notches occurred. Moreover, with the blocked configuration the notches were still present, although smaller, at approximately the same frequencies. Therefore, it is unlikely that ear-bar resonances were responsible for the notches. In addition, alterations to the cochlea, such as acoustic trauma, have been shown to change the depth of these notches (Nakajima, 1991). Therefore, it seems that the source of the notches originates within the cochlea. Because the blocked ear-bar configuration resulted in a smoother frequency response, measurements of the emissions were performed with this configuration when acoustic stimulation was unnecessary.

II. RESULTS

A. Electrically evoked emission frequency response

Figure 4 shows the electrically evoked emission's frequency responses for three turn-3 experiments and for three turn-2 experiments. The CFs of the electrode locations are
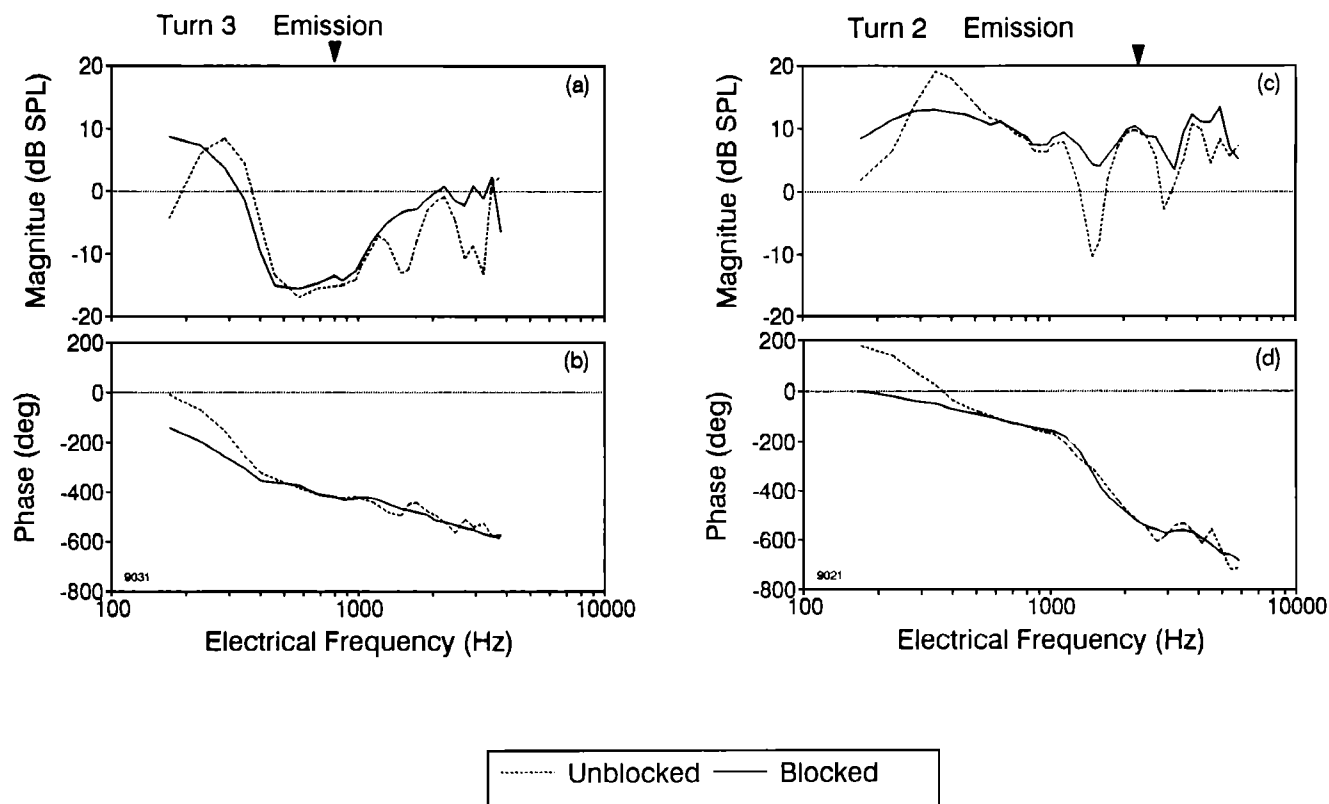
FIG. 2. The turn-3 and turn-2 electrically evoked emission frequency responses for the blocked and unblocked acoustic loads. The electrical current levels were approximately 10 and 12 μA for animals 9031 (turn 3) and 9021 (turn 2), respectively.

indicated by the arrows at the top of the plots. Turn-2 responses exhibited greater interanimal variability than those of turn 3. When the electrode was in turn 3, the major minimum in emission magnitude (to approximately 0 dB SPL) occurred between the frequencies of 500 and 1000 Hz. In turn-2 experiments, the local minima in magnitude occurred at frequencies between 1.5 and 3 kHz. In both turns, these minima occurred near the CF of the electrode location. In addition, the turn-2 magnitude responses exhibited a consistent small notch across animals at approximately 1 kHz [Fig. 4(c)]. The 3-dB cutoff frequency for the relatively large emissions below the major notch is between 300 and 350 Hz for turn 3 and at approximately 2 kHz for turn 2.

The phase response curves were similar across animals for each turn [Fig. 4(b) and (d)]. However, there were considerable differences in the phase responses between turn-3 and turn-2 electrode locations. For each turn, comparison between the magnitude and phase response curves shows that fluctuations in the magnitude data often occurred at the same frequencies where the phase exhibited fluctuations.

Examples of phase data for turn 3 and for turn 2 are plotted on a linear frequency scale in Fig. 5. This figure was obtained by choosing a representative phase response for turn 3 and turn 2 (experiment 9024 and 9027, respectively) from Fig. 4(b) and (d). The turn-3 phase response at frequencies, 200 to 500 Hz, exhibits a greater phase lag with frequency than at higher frequencies. The low-frequency region is below the frequency where the major minimum in magnitude occurs. The higher frequency region, where the phase

changes only slightly with frequency, corresponds to the frequencies above the magnitude response's major minimum. The turn-2 phase response also has two separate slopes (one for low and one for high frequencies), but there is a wider low-frequency range (200 Hz to 2.5 kHz) where the phase changes relatively rapidly with frequency. The rate of change in phase response of low-frequency turn-2 emissions is less than that of low-frequency turn-3 emissions. The break point between the low-frequency slope and the high-frequency slope occurs slightly below the CF of each electrode location.

The group delay, $\tau(\omega)$, of a linear time-invariant system is the negative of the slope of the phase curve. The group delay (in seconds) of a system is defined as $\tau(\omega) = -d\phi(\omega)/d\omega$, where ϕ is the phase angle in radians and ω is the frequency in rad/s for a continuous phase response (Oppenheim and Schafer, 1989). The linear phase-response regions support the idea that the electrically evoked emissions propagate to the stapes as a reverse traveling wave. By calculating the group delay from the phase response, we estimate the travel time of the emission from its place of generation to the place of measurement at the eardrum. The phase responses show two regions in which the phase varies approximately linearly with frequency. This corresponds to two group delays, one for frequencies below, the other for frequencies above the CF of the electrode location. Linear-regression lines were calculated for both low-frequency and high-frequency regions for each turn, as shown in Fig. 5. For turn 3, one slope was calculated for frequencies between 172 and

Nakajima et al.: Electrically evoked otoacoustic emissions
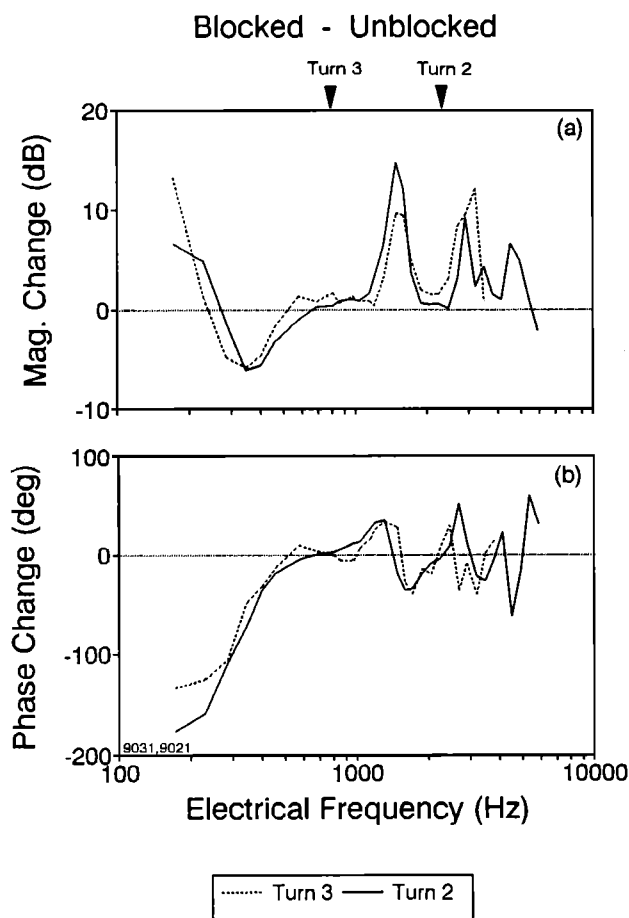
Blocked - Unblocked

FIG. 3. The change in emission frequency responses between the blocked and unblocked case for turn 3 and turn 2. (a) The magnitude change was calculated as the difference in decibels (blocked–unblocked). (b) The phase change was calculated separately as the difference in degrees (blocked–unblocked).

460 Hz, and one for frequencies between 574 Hz and 4.94 kHz. For turn 2, slopes were calculated for frequencies between 172 Hz and 2.47 kHz, and for frequencies between 2.7 and 4.94 kHz. The estimated group-delay values are indicated next to the estimated lines in Fig. 5 for the two representative experiments. Average estimated group delays were obtained from four turn-3 animals and five turn-2 animals. When the electrode was in turn 3, the low-frequency slope of the phase versus frequency corresponded to an average group delay of 2.52±0.229 ms for emissions between 172 and 460 Hz. The average turn-3 group delay for frequencies between 574 Hz and 4.94 kHz was 0.15±0.002 ms. When the electrode was in turn 2, averaged group delay for emissions from 172 Hz to 2.47 kHz was 0.65±0.043 ms, and for emissions between 2.7 and 4.94 kHz the averaged group delay was 0.17±0.116 ms.

If the low-frequency linear regression lines in Fig. 5 are extrapolated to the y-axis, the y-intercepts of the lines give us predictions for the phases at very low frequencies. The average y-intercept was 22±42.7 deg for low-frequency turn-3 slope and 32±12.1 deg for the turn-2 slope.

B. The effect of death

Overdose with sodium pentobarbital resulted in death, defined for our purposes as cardiac arrest accompanied by the rapid decrease in EP in the scala media from approximately 90 to −10 mV. The magnitude and phase of electrically evoked emissions changed considerably after the death of the animal, and eventually the emission magnitude fell to the noise level. The CM magnitude also decreased after the death of the animal.

Figure 6 shows the electrically evoked emissions measured before and after death for an experiment with the microelectrode located in turn 3. The times on the legends are relative to the time of death. The initial recording before death is represented with closed squares. Death initially caused an increase in emission magnitude at low frequencies (approximately 200 to 700 Hz) and a decrease at high frequencies (approximately 1 to 3 kHz). About 1 h after death (open square data points), the emission magnitude decreased for most frequencies and dropped to the noise floor after approximately 3 h. The high-frequency electrically evoked emission measurements changed little after death. For example, emission magnitudes above 3.5 kHz in Fig. 6(a) changed much less after death compared to the lower frequencies. The phase at high frequencies exhibited little change after death until the emissions fell to the noise level, after 3 h.

Figure 7 shows the input-output curves for the 195 Hz CM, recorded at approximately the same time as the emission data in Fig. 6. The initial recording before death is represented with the closed square markers and the legend indicates the time relative to the time of death in hours. After death, the CM initially decreased by approximately 10 dB. This corresponds to the time period when the emission magnitude made its initial increase. An hour after death, the CM at higher sound levels dropped an additional 10 to 30 dB. By this time, the emissions had also decreased.

III. DISCUSSION

The frequency response of electrically evoked emissions is dependent on the location of the current-stimulating electrode. At each electrode frequency location, the largest magnitudes occur at frequencies below the CF of the electrode locations. This is consistent with previous studies in the gerbil (Mountain and Hubbard, 1989), but we are now able to make more detailed recordings that include higher frequencies. We now find that at frequencies above the CF of the electrode location the emissions increase, thus resulting in a local minimum near the CF of the electrode location. Increases in magnitude at high frequency may be indicative of the stimulus current leaking across turns within the cochlea from turn 3 to turn 2 and from turn 2 to turn 1. Thus the current may be stimulating higher frequency locations.

Comparison of our data with that of Murata et al. (1991), who measured turn-2 and turn-3 electrically evoked emission magnitudes in the guinea pig, show both similarities and differences. Their magnitude responses resemble our responses measured with the unblocked acoustic configuration for turn 2. Their turn-2 response had a notch (local minimum) between 1.5 and 2 kHz. However, overall their response curves had a low-pass character with the magnitude cutoff frequency at approximately 3 kHz for turn 2. Our turn-3 magnitude has an initial cutoff at approximately 300
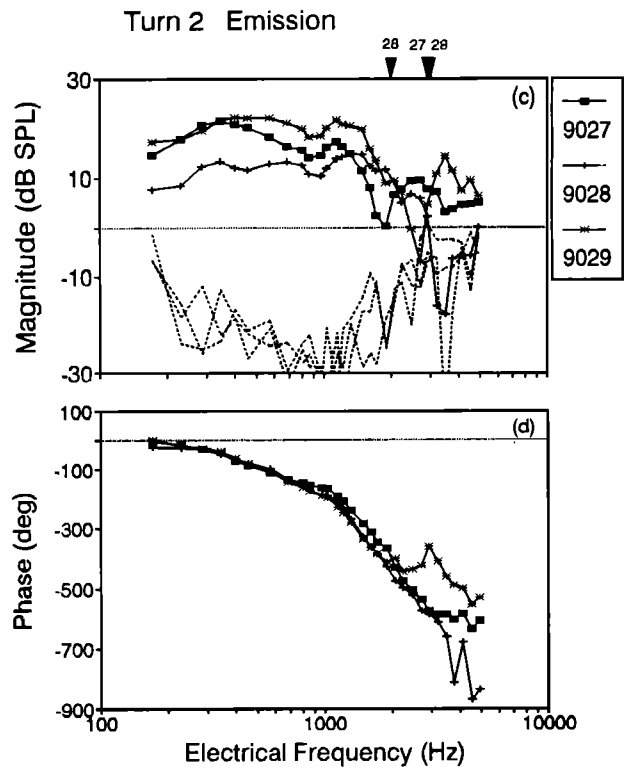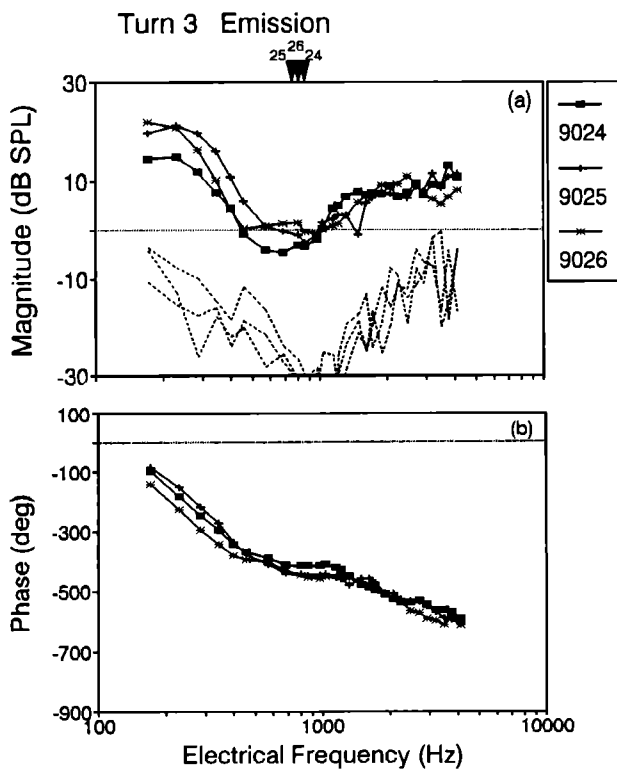
FIG. 4. Emission frequency responses of three animals for turn 3 [(a) and (b)] and three animals for turn 2 [(c) and (d)]. The arrows at the top indicate the characteristic frequencies of the electrode locations. The dashed lines in the magnitude responses represent the noise measurements. All measurements were performed with the blocked ear-bar configuration and the electrical current level was approximately 12 μA.

Hz and then increases at higher frequencies. Murata *et al.*'s turn-3 magnitude cuts off at approximately 1 kHz. Their magnitude responses did not increase for higher frequency stimulation. It is possible that they would have observed an emission increase at high frequency if they had used higher frequency stimuli.

Species-related differences in current leakage across turns could explain the differences between our data and that of Murata *et al.* In the chinchilla, Ronken and Eldredge
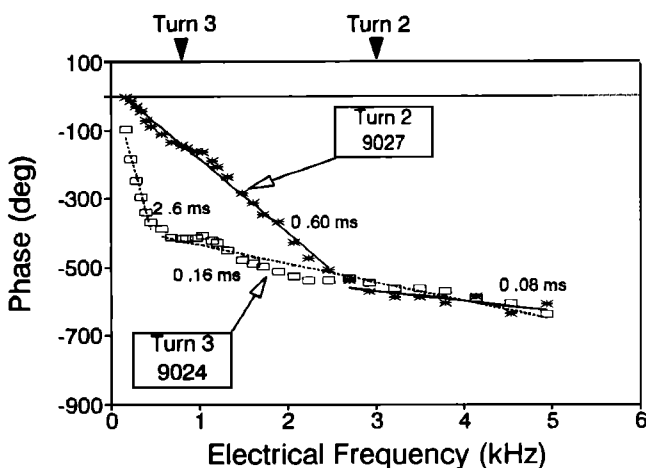
FIG. 5. An example of the linear regression analysis used to calculate the group delay of the emission data. Data from both turns were fit by two straight-line segments. The values next to the lines indicate the estimated group delay. Turn-3 phase (experiment 9024) and turn-2 phase (experiment 9027) data are representative animals from Fig. 4.
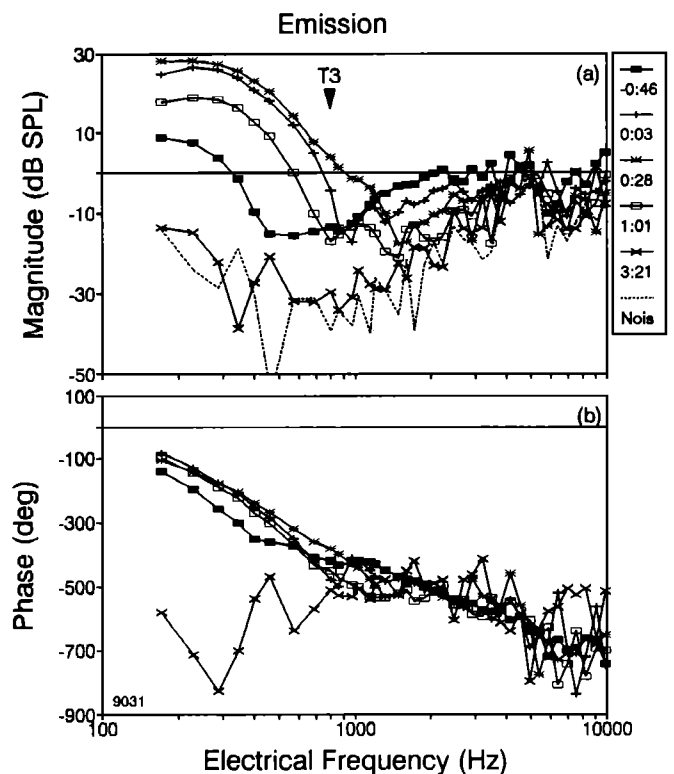
FIG. 6. The effect of death on the emission frequency responses. The response before death is plotted with closed square data points. The legend gives the time when the data is taken relative to the time of death in hours:minutes. The dashed line in panel (a) represents the noise level. The electrical current level was approximately 10 μA. Data are from a turn-3 experiment using the blocked ear-bar configuration.

Cochlear Microphonic
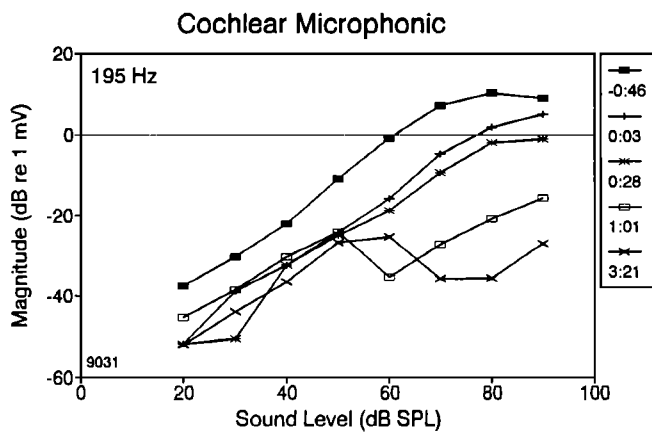
FIG. 7. The effect of death on the 195 Hz CM input–output curves. These measurements were recorded at approximately the same time as the emission data in Fig. 6. The times indicated represent the beginning of the emission recording time. The CM was recorded approximately 14 min after each emission recording.

FIG. 8. A conceptual feedback model of the cochlea adapted from Hubbard and Mountain (1990). The outer hair cells are represented by two separate processes: mechanoelectric transduction and electromechanical transduction. The diagram shows that acoustic input produces CM via the mechano-electric transduction process. Electrical current produces otoacoustic emissions via the electromechanical transduction process. Acoustic trauma or changes in EP can lead to the opening of the feedback loop by decreasing the gain of the mechanoelectric transduction mechanism, while electromechanical transduction is still intact.

(1981) observed that CM leakage across turns was possible. The gerbil cochleas in our experiments may exhibit some current leakage across turns resulting in the increased magnitudes at high frequencies, whereas the guinea pig cochleas in Murata et al.'s experiments may not.

In addition, Murata et al.'s experimental procedure differed from ours in several ways which could account for the differences in results. They used current levels of 20 to 100 μA while we used 10 to 15 μA. We have preliminary data which indicate that the emission frequency response can be altered by high current levels. The impedance of their acoustic system was likely different from ours. As we have shown in Fig. 2, differences in acoustic-system impedance can have a significant effect in the emission frequency response. In addition, they could not monitor cochlear condition with EP measurements because they used a metal electrode. In our experience, emissions obtained from high-EP cochleas differed greatly from low-EP cochleas (Nakajima, 1991). Moreover, Murata et al. used click-evoked N_1 instead of the more frequency-specific tone-evoked N_1 to monitor cochlear condition. We have shown that changes in tone-evoked N_1 are associated with changes in emission frequency response (Nakajima, 1991; Nakajima et al., 1991).

Electrically evoked emission response exhibited notable changes after the death of an animal. Shortly after the cessation of the heart beat, there was a very rapid drop in EP accompanied by a slower drop in CM. The low-frequency emissions increased and the high-frequency emissions decreased after death. Murata et al. (1991) also showed a single case of death precipitating an increase in guinea-pig electrically evoked otoacoustic emission at 170 Hz. The observation that electrically evoked emission magnitudes could increase and remain constant for many minutes after death suggests that electromechanical transduction can survive after the death of the animal, even when the mechanoelectric transduction is compromised.

Other types of manipulations such as furosemide injection, which reduces EP and CM, also result in the increase of low-frequency electrically evoked emissions (Hubbard and

Mountain, 1990). The enhancement of low-frequency emissions could be the result of opening the feedback loop in a negative feedback system similar to the model depicted in Fig. 8. Manipulations such as furosemide injection and death decrease the EP which provides much of the driving force for mechanoelectric transduction. The reduction in mechanoelectric transduction opens the loop, thus increasing the emission response by a factor of up to one plus the loop gain (Mountain and Hubbard, 1989). Hubbard and Mountain (1990) found that furosemide injection results in an emission increase of 12 dB, which corresponds to a loop gain of at least three (for turn-2 emissions at 600 Hz). Here, we find that death can result in an emission increase of 19.4 dB (at 172 Hz for turn 3), indicating a loop gain of at least eight. Acoustic trauma which decreases CM, indicating damage to mechanoelectric transduction, also results in increased low-frequency emission magnitudes (Hubbard et al., 1990; Nakajima et al., 1991). Finally, simultaneous acoustic stimulation, which may saturate mechanoelectric transduction (effectively "opening the loop"), also results in 15-dB enhancement of turn-2 (450 Hz) electrically evoked emission, corresponding to a loop gain of at least four (Mountain and Hubbard, 1989).

Other investigators have studied otoacoustic emissions with compromised cochleas. The acoustically evoked distortion products in the gerbil have been shown to persist up to 2 h after death from anoxia (Schmiedt and Adams, 1981). They found that the cubic difference tone $(2f_1-f_2)$ decreases initially, then recovers to approximately the normal magnitude. The difference tone (f_2-f_1) was found to actually increase over 10 dB after anoxia. Both types of distortion products were found to decrease after 30 min following anoxia. However, Kemp and Brown (1984) found gerbil cubic difference distortion product emissions $(2f_1-f_2)$ to decline 5 to 10 min after death. Schmiedt (1986) later noted that the effect on $2f_1-f_2$ distortion product due to anoxia is dependent on the levels of the stimuli. Lonsbury-Martin et al. (1987) found

that stimulus level of 75 dB SPL produced distortion products that lasted longer after death than the 65 dB SPL evoked emissions. They found this pattern to be true for the distortion product $2f_1 - f_2$ and the odd-order intermodulation distortion product $2f_2 - f_1$ in the rabbit. Whitehead *et al.* (1992) also noted similar characteristics in the rabbit where $2f_1 - f_2$ distortion products were affected by lethal anoxia, injection of ethacrynic acid, or ethacrynic acid plus gentamicin. The cubic distortion product was severely affected if <60–70 dB SPL stimuli was used and less affected with >60–70 dB SPL stimuli. Recently, Rebillard and Lavigne-Rebillard (1992) observed that after hypoxia $2f_1 - f_2$ emissions in the guinea pig often initially increase (4 dB) then decrease. Mills *et al.* (1993) showed that the temporary decrease in EP due to furosemide injection resulted in a decrease then recovery to near normal magnitude for the odd distortion product emissions $(2f_1 - f_2)$, $(3f_1 - 2f_2)$, and $(2f_2 - f_1)$. The even-order term $(f_2 - f_1)$ responded in a less consistent manner, eventually recovering to near normal. One example of the $2f_1 - f_2$ term evoked by 50 dB SPL stimuli showed a tendency to overshoot (approximately 2 dB) after recovery. Although distortion product emissions may involve a different generation mechanism from that of the electrically evoked emissions, it is interesting that both types of emissions have been noted to persist and even increase shortly after the death of an animal.

Knowledge of the electrically evoked otoacoustic emission phase responses in the blocked ear-bar case allows us to infer the polarity of pressure changes within the cochlea due to electrical stimulation. The average y-intercept for the emission phase versus frequency plot was near 0° with respect to condensation. For low frequencies, we expect that the pressure measured at the tympanic membrane is proportional to the pressure in the scala vestibuli. This suggests that when a positive current is injected into the scala media, the OHC mechanical response results in a positive pressure in the scala vestibuli at the stapes.

The middle ear could introduce a phase shift between the pressure in the scala vestibuli and the pressure measured at the tympanic membrane if the impedance looking into the acoustic system from the ear canal is comparable to, or lower than, the impedance of the middle ear. Such appears to be the case with the unblocked ear bar (Fig. 2) in which a relative phase lead is seen for frequencies below 500 Hz. When the impedance of the acoustic system is significantly increased (blocked ear bar), then the phase lead is reduced by 130°–180°. If we assume that the phase of the scala vestibuli pressure remains unchanged, then these results suggest that the blocked ear-bar configuration significantly reduces the phase shift introduced by the middle ear.

A similar phase lead can also be seen in the data of Xue *et al.* (1993b) who used an acoustic system very similar to our unblocked system. They compared electrically evoked basilar membrane motion in the hook region to the electrically evoked emission and found that below 700 Hz the emission could exhibit as much as 200° lead with respect to basilar membrane velocity. This phase shift introduced by the middle ear appears to be important only at low frequencies, since they found that from 700 Hz to 10 kHz both the magnitude and the phase of the emission matched that of the basilar membrane velocity if the emission data were corrected for a 49-μs travel time to the probe-tube microphone.

The group delays and low-frequency intercepts in the present study are based on phase data measured with the high-impedance system. With this system the phase shifts introduced by the middle ear should be quite small and would not be expected to influence the group delay estimates. The middle ear effect may, however, explain the small phase lead observed in the low-frequency intercept.

Both the electrically evoked emission and the CM are distributed responses. The space constant for the electrically evoked emission was estimated to be 1.5 mm by Xue *et al.* (1993a). At low frequencies, the wavelength of the generated wave on the basilar membrane is far greater than the space constant, thus the interpretation of the phase measurements should be reasonably accurate.

The calculations of group delays from acoustically evoked CM data and electrically evoked emissions suggest that different modes are stimulated preferentially for acoustic and electrical stimulation. Schmiedt and Zwislocki (1977) estimated travel times by measuring the low-frequency group delay derived from the CM phase measured in turn 2 and turn 3 of an open-bulla cochlea of a gerbil. The CM phase was calculated relative to the CM phase measured near the stapes. The travel times they estimated were approximately 1 ms for the turn-3 region and 0.3 ms for the turn-2 region. From the low-frequency regions, where the emissions are relatively large (to 500 Hz for turn 3, and to 2.5 kHz for turn 2), the electrically evoked emissions have estimated group delays of 2.5 ms (turn 3) and 0.7 ms (turn 2). A comparison between our data and that of Schmiedt and Zwislocki indicates that the electrically evoked-emission travel time is at least twice the travel time of the acoustically evoked CM response. The difference in group delays suggests that electrical simulation and acoustic stimulation may preferentially excite different propagation modes. The possibility of two modes is particularly intriguing because the recent model by Hubbard (1993) requires two coupled propagation modes. With the original model parameters, propagation mode velocities differ by a factor of 2 in the midcochlear region (turn 2) and by a factor of 20 in the base. The direct comparison to the present experimental data is not possible because the traveling-wave model has not yet been developed to the stage of simulating electrically evoked emissions.

High-frequency turn-3 emissions (between 500 Hz and 5 kHz) and high-frequency turn-2 emission (between 2.5 kHz and 5 kHz) have nearly equal group delays of approximately 0.16 ms. The disparity between group delays at high frequencies and low frequencies for each turn may result from phase cancellation at high frequencies where the wavelength approaches the space constant of the electrical current spread. An alternative possibility is that the high-frequency emissions have originated from areas closer to the base, thus producing shorter delays. This is consistent with the possibility that some of the current leaks to the basal turns of the cochlea, therefore stimulating higher frequency regions.

Otoacoustic emissions, electrically evoked from both turn 2 and turn 3 of the gerbil cochlea, (i) have a complex frequency dependence, and (ii) seem to emerge from the co-

793   J. Acoust. Soc. Am., Vol. 96, No. 2, Pt. 1, August 1994

Nakajima *et al.*: Electrically evoked otoacoustic emissions   793

chlea with two distinct group delays. Both of these features vary with the stimulation site, but are consistent between animals. The group delays for the reverse traveling wave that correspond to the most robust electrically evoked emissions for each turn are longer (by at least a factor of two) than the delays that have been measured by others for the acoustically evoked forward traveling wave. The existence of two significant propagation modes in the cochlea would pose a major challenge to most existing theories of cochlear function.

ACKNOWLEDGMENTS

Ashmore, J. F. (**1987**). "A fast motile response in guinea pig outer hair cells: the cellular basis of the cochlear amplifier," J. Physiol. **388**, 323–347.

Brownell, W. E., Bader, C. R. Bertrand, D., and de Ribaupierre, Y. (**1985**). "Evoked mechanical responses of isolated cochlear outer hair cells," Science **277**, 194–196.

Cody, A. R., and Russell, I. J. (**1987**). "The response of hair cells in the basal turn of the guinea pig cochlea to tones," J. Physiol. **383**, 551–569.

Dallos, P. (**1985**). "Response characteristics of mammalian cochlear hair cells," J. Neurosci. **5**, 1591–1608.

Dallos, P. (**1986**). "Neurobiology of cochlear inner and outer hair cells: intracellular recordings," Hear. Res. **22**, 185–198.

Dallos, P., Santos-Sacchi, J., and Flock, A. (**1982**). "Intracellular recordings from cochlear outer hair cells," Science **218**, 582–584.

Davis, H. (**1983**). "An active process in cochlear mechanics," Hear. Res. **9**, 79–90.

Fahey, P. F., and Allen, J. B. (**1985**). "Characterization of cubic intermodulation distortion products in the cat external auditory meatus," in *Peripheral Auditory Mechanisms* edited by J. B. Allen, J. L. Hall, A. E. Hubbard, S. R. Neely, and A. Tubis (Springer-Verlag, New York), pp. 314–321.

Hubbard, A. E. (**1993**). "A traveling-wave amplifier model of the cochlea," Science **259**, 68–71.

Hubbard, A. E., and Mountain, D. C. (**1983**). "Alternating current delivered into the scala media alters sound pressure at the eardrum," Science **222**, 510–512.

Hubbard, A. E., and Mountain, D. C. (**1990**). "Haircell forward and reverse transduction: Differential suppression and enhancement," Hear. Res. **43**, 269–272.

Hubbard, A. E., Nakajima, H. H., Olson, E. S., and Mountain, D. C. (**1990**). "Sound induced changes in electrically evoked cochlear emissions," in *The Mechanics and Biophysics of Hearing* edited by P. Dallos, C. D. Geisler, J. W. Matthew, M. A. Ruggero, and C. R. Steele (Springer-Verlag, New York), pp. 186–193.

Kemp, D. T., and Brown, A. M. (**1984**). "Ear canal acoustic and round window electrical correlates of $2f_1-f_2$ distortion generated in the cochlea," Hear. Res. **13**, 39–46.

Kössl, M., and Russell, I. J. (**1992**). "The phase and magnitude of hair cell receptor potentials and frequency tuning in the guinea pig cochlea," J. Neurosci. **12**, 1575–1586.

Lonsbury-Martin, B. L., Martin, G. K., Probst, R., and Coats, A. C. (**1987**). "Acoustic distortion products in rabbit ear canal. I. Basic features and physiological vulnerability," Hear. Res. **28**, 173–189.

Matthews, J. W. (**1983**). "Modeling reverse middle ear transmission of acoustic distortion signals," in *Mechanics of Hearing*, edited by E. de Boer and M. A. Viergever (Delft U.P., Delft), pp. 11–18.

Mills, D. M., Norton, S. J., and Rubel, E. W. (**1993**). "Vulnerability and adaptation of distortion product otoacoustic emission to endocochlear potential variation," J. Acoust. Soc. Am. **94**, 2108–2122.

Mountain, D. C., and Hubbard, A. E. (**1989**). "Rapid force production in the cochlea," Hear. Res. **42**, 195–202.

Mountain, D. C., Hubbard, A. E., and McMullen, T. A. (**1983**). "Electromechanical processes in the cochlea," in *Mechanics of Hearing*, edited by E. de Boer and M. A. Viergever (Delft U.P., Delft), pp. 119–126.

Murata, K., Moriyama, T., Hosokawa, Y., and Minami, S. (**1991**). "Alternating current induced otoacoustic emissions in the guinea pig," Hear. Res. **55**, 201–214.

Nakajima, H. H. (**1991**). "A study of the electromechanical properties of the cochlea utilizing electrically evoked emissions and acoustic trauma," MS thesis, Boston University, Boston, MA.

Nakajima, H. H., Olson, E. S., Mountain, D. C., and Hubbard, A. E. (**1991**). "Electrically evoked emissions and acoustic trauma," in *Proceedings of the 1991 IEEE Seventeenth Annual Northeast Bioengineering Conference*, edited by M. D. Fox, M. A. F. Epstein, R. B. Davis, and T. M. Alward (IEEE, New York), pp. 213–214.

Oppenheim, A. V., and Schafer, R. W. (**1989**). *Discrete-Time Signal Processing* (Prentice-Hall, New Jersey).

Rebillard, G., and Lavigne-Rebillard, M. (**1992**). "Effect of reversible hypoxia on the compared time courses of endocochlear potential and $2f_1-f_2$ distortion products," Hear. Res. **62**, 142–148.

Rhode, W. S. (**1971**). "Observations of the vibration of the basilar membrane in squirrel monkeys using the Mössbauer technique," J. Acoust. Soc. Am. **49**, 1218–1231.

Rhode, W. S. (**1973**). "An investigation of post-mortem cochlear mechanics using the Mössbauer effect," in *Basic Mechanisms in Hearing*, edited by A. R. Möller (Academic, New York and London), pp. 49–63.

Rhode, W. S. (**1978**). "Some observations on cochlear mechanics," J. Acoust. Soc. Am. **64**, 158–176.

Ronken, D. A., and Eldredge, D. H. (**1981**). "Identification of local and propagating distortion products from cochlear microphonic responses," J. Acoust. Soc. Am. **70**, 410–425.

Russell, I. J., and Sellick, P. M. (**1978**). "Intracellular studies of hair cells in the mammalian cochlea," J. Physiol. **284**, 261–290.

Schmiedt, R. A. (**1986**). "Effects of asphyxia on levels of ear canal emissions in gerbil," Abstr. Assoc. Res. Otolaryngol. **9**, 112–113.

Schmiedt, R. A., and Adams, J. C. (**1981**). "Stimulated acoustic emissions in the ear canal of the gerbil," Hear. Res. **5**, 295–305.

Schmiedt, R. A., and Zwislocki, J. J. (**1977**). "Comparison of sound-transmission and cochlear-microphonic characteristics in Mongolian gerbil and guinea pig," J. Acoust. Soc. Am. **61**, 133–149.

Sellick, P. M., Patuzzi, R., and Johnstone, B. M. (**1982**). "Measurement of basilar membrane motion in the guinea pig using the Mössbauer technique," J. Acoust. Soc. Am. **72**, 131–141.

Whitehead, M. L., Lonsbury-Martin, B. L., and Martin, G. K. (**1992**). "Evidence for two discrete sources of $2f_1-f_2$ distortion-product otoacoustic emission in rabbit. II: Differential physiological vulnerability," J. Acoust. Soc. Am. **92**, 2662–2682.

Xue, S., Mountain, D. C., and Hubbard, A. E. (**1993a**). "Acoustic enhancement of electrically-evoked otoacoustic emission reflects basilar membrane tuning: Experiment results," Hear. Res. **70**, 121–126.

Xue, S., Mountain, D. C., and Hubbard, A. E. (**1993b**). "Direct measurement of electrically-evoked basilar membrane motion," in *Biophysics of Hair Cell Sensory Systems* edited by H. Duifhuis, J. W. Horst, P. van Dijk, and S. van Netten (World Scientific, Singapore), pp. 361–369.

Zwicker, E. (**1990**). "On the influence of acoustical probe impedance on evoked otoacoustic emissions," Hear. Res. **47**, 185–190.